

This discussion paper is/has been under review for the journal Atmospheric Chemistry and Physics (ACP). Please refer to the corresponding final paper in ACP if available.

Vorticity budget in Typhoon Nuri

D. J. Raymond and
C. López Carrillo

The vorticity budget of developing Typhoon Nuri (2008)

D. J. Raymond and C. López Carrillo

Physics Department and Geophysical Research Center, New Mexico Tech, Socorro, NM, USA

Received: 20 April 2010 – Accepted: 18 June 2010 – Published: 2 July 2010

Correspondence to: D. J. Raymond (raymond@kestrel.nmt.edu)

Published by Copernicus Publications on behalf of the European Geosciences Union.

Title Page

Abstract

Introduction

Conclusions

References

Tables

Figures

⏪

⏩

◀

▶

Back

Close

Full Screen / Esc

Printer-friendly Version

Interactive Discussion



Abstract

The formation of west Pacific tropical cyclone Nuri (2008) was observed over four days from easterly wave to typhoon stage by aircraft using scanning Doppler radar and dropsonde data. This typhoon intensified rapidly in a significantly sheared environment. In spite of the shear, overlapping closed circulations existed in the storm frame of reference in the boundary layer and at 5 km elevation, providing a deep region protected from environmental influences. The vorticity budget was analyzed and it was found that vorticity convergence dominated vortex tilting on the storm scale in the lower troposphere. At times vorticity convergence also greatly exceeded frictional spindown in the boundary layer. Thus, the Ekman pumping hypothesis was found to be a poor approximation in the early stages of the development of this typhoon. As Nuri developed, convective sources of boundary layer vorticity became fewer but more intense, culminating in a single nascent eyewall at the tropical storm stage. A non-developing tropical wave case was also analyzed. This system started with much weaker circulations in the boundary layer and aloft, leaving it unprotected against environmental intrusion. This may explain its failure to develop.

1 Introduction

A detailed accounting of the vorticity budget of a developing tropical cyclone is necessary to understand how the storm spins up. Measurements from a recent field program are used here to clarify this budget during the formation and intensification of Typhoon Nuri (2008) and in a non-developing tropical wave.

The full vorticity equation in flux form (Haynes and McIntyre, 1987) is

$$\begin{aligned}\frac{\partial \zeta_z}{\partial t} &= -\nabla_h \cdot (\mathbf{v}_h \zeta_z - \zeta_h \mathbf{v}_z + \hat{\mathbf{k}} \times \mathbf{F}) \\ &= -\nabla_h \cdot (\mathbf{Z}_1 + \mathbf{Z}_2 + \mathbf{Z}_f),\end{aligned}\quad (1)$$

Vorticity budget in Typhoon Nuri

D. J. Raymond and
C. López Carrillo

Title Page

Abstract

Introduction

Conclusions

References

Tables

Figures

◀

▶

◀

▶

Back

Close

Full Screen / Esc

Printer-friendly Version

Interactive Discussion



where ζ_z is the vertical component of absolute vorticity, ∇_h is the horizontal (i.e., constant geometric height) divergence, \mathbf{v}_h and v_z are the horizontal and vertical components of the wind, ζ_h is the horizontal vorticity component, and $\hat{\mathbf{k}}$ is the vertical unit vector. The quantity Z_1 is the advective flux of vorticity, Z_2 is the vorticity flux associated with vortex tilting, and Z_f is the flux of vorticity due to the force F associated with the divergence of the Reynolds stress. This force is generally thought to be due primarily to surface friction. The terms Z_2 and Z_f are together called the non-advective flux of vorticity.

The convergence of the advective flux Z_1 can be split into two pieces,

$$-\nabla_h \cdot Z_1 = -\mathbf{v}_h \cdot \nabla_h \zeta_z - \zeta_z \nabla_h \cdot \mathbf{v}_h, \quad (2)$$

the first of which simply advects vorticity around and the second of which modifies vorticity via vertical stretching. Advection does not change the magnitude of vorticity in a parcel; this role is reserved for the second term, commonly called the stretching term, which can increase or decrease the magnitude of vorticity (but not change the sign).

Many simplified models of tropical cyclones, (e.g., Ooyama, 1969) and successors, assume Ekman balance in the boundary layer of a developing cyclone. Ekman balance is an extension of geostrophic balance in which the pressure gradient force, the Coriolis force, and surface friction are assumed to sum to zero. Since the addition of friction to the mix results in flow down the pressure gradient, this assumption produces mass convergence in regions of low pressure, such as the core of a developing tropical cyclone. This convergence is postulated to drive the convection in the cyclone.

Smith and Montgomery (2008) evaluate the validity of a number of balance approximations, including Ekman balance, against a steady-state boundary layer model based on the full primitive equations. They find that many of these approximations are not justified in the inflow region of a tropical cyclone.

This issue is finessed here by considering not the primitive equations directly, but the vorticity equation. Postulating a steady state flow in which the tilting term $Z_2 = -\zeta_h v_z$ is

Vorticity budget in Typhoon Nuri

D. J. Raymond and
C. López Carrillo

Title Page

Abstract

Introduction

Conclusions

References

Tables

Figures



Back

Close

Full Screen / Esc

Printer-friendly Version

Interactive Discussion



ignored in the vorticity equation leads (with minor rearrangement) to a balance between the divergence of absolute vorticity and the curl of surface friction:

$$\nabla_h \cdot (\mathbf{v}_h \zeta_z) = \hat{\mathbf{k}} \cdot \nabla \times \mathbf{F}. \quad (3)$$

This *vorticity balance* is related to, but is not identical to Ekman balance, as it incorporates advection terms from the momentum equation in addition to the Coriolis force and friction terms. In any case it is this balance, when evaluated in a storm-relative frame, which applies to a steady or nearly steady tropical cyclone if vortex tilting is insignificant. Whether vorticity balance is a valid approximation in the developing stage of a tropical cyclone is a theme of this paper. The issue is important because, as Zehnder (2001) shows, the imposition of such a balance has major implications for storm intensification.

Developing tropical systems often first exhibit significant cyclonic vorticity at middle levels in the troposphere (Ritchie and Holland, 1997; Bister and Emanuel, 1997; Raymond et al., 1998). However, the development of strong near-surface vorticity is necessary for the amplification of the cyclone vortex and the initiation of the cyclone heat engine (Emanuel, 1986). An important problem is then to understand how the surface vortex develops.

Ritchie and Holland (1997) assert that mid-level vortex merger leads to downward vortex development, but do not explain how this might occur. Potential vorticity anomalies with larger horizontal scale exhibit greater vertical penetration. Quasi-geostrophic calculations of this effect for the vortices described in their paper suggest that the increased penetration is minimal, but as Davis (1992) has shown, stronger vortices in the nonlinear balance regime exhibit greater vertical penetration than quasi-geostrophic calculations would suggest.

Bister and Emanuel (1997) argue that the development of a cool, moist environment resulting from stratiform rain serves as the incubation region for the formation of a low-level, warm-core vortex. They also assert that downdrafts associated with mesoscale rain areas advect the mid-level vortex downward, thus increasing low-level vorticity.

Vorticity budget in Typhoon Nuri

D. J. Raymond and
C. López Carrillo

Title Page

Abstract

Introduction

Conclusions

References

Tables

Figures

◀

▶

◀

▶

Back

Close

Full Screen / Esc

Printer-friendly Version

Interactive Discussion



In terms of the flux form of the vorticity equation, what is probably happening in their model is that the tilting term on the right side of Eq. (1) $Z_2 = -\zeta_h v_z \approx -\hat{k} \times (\partial \mathbf{v}_h / \partial z) v_z$ acts to advect mid-level momentum downward to low levels. Such momentum transport would produce vertical vorticity dipoles, with neighboring regions of positive and negative vorticity. In axial symmetry, this would produce a central region of elevated vorticity surrounded by a ring of depressed (or negative) vorticity, such that the circulation around the entire system remains unchanged.

Raymond et al. (1998) attempted to account for the observed spinup of tropical cyclones in the east Pacific using airborne Doppler radar data. The primary mechanism for spinup was assumed to be vorticity convergence, represented by the first term on the right side of (1). Observed convergence was sufficient to overcome frictional spin-down (the third term on the right side of (1)) in the very earliest stages of spinup when the disturbance was still a wave or a weak tropical depression. However, in the tropical storm stage the estimated vorticity convergence was unable to overcome friction unless the surface stress was distributed vertically over several kilometers by deep convection. A significant weakness of this analysis is that the vorticity in the convergence term was assumed to be approximately equal to the planetary vorticity, i.e., the Coriolis parameter. As we shall see, this may be a plausible assumption in the very earliest stages, but it is incorrect in the tropical storm stage.

Assuming that convergence of low-level vorticity is the most important mechanism for spinning up a tropical cyclone, how much of this convergence is the result of widespread, ordinary convection and how much of it occurs in strong but isolated convective systems? The overall circulation tendency around the cyclone doesn't depend on how vorticity convergence is distributed within the circulation loop, but the internal structure of the system does.

Hendricks et al. (2004) and Montgomery et al. (2006) present evidence that strong, isolated convection prevails, and denote these strong convective systems vortical hot towers (VHTs). The updrafts of VHTs are rotating rapidly and Hendricks et al. (2004) suggest that this rotation may be strong enough to suppress entrainment and thus

Vorticity budget in Typhoon Nuri

D. J. Raymond and
C. López Carrillo

[Title Page](#)[Abstract](#)[Introduction](#)[Conclusions](#)[References](#)[Tables](#)[Figures](#)[⏪](#)[⏩](#)[◀](#)[▶](#)[Back](#)[Close](#)[Full Screen / Esc](#)[Printer-friendly Version](#)[Interactive Discussion](#)

alter the vertical mass flux profile of VHTs compared to more mundane forms of deep tropical convection. Furthermore, the core of the developing tropical cyclone appears to form from the merger of the residual vortices left by VHTs.

Since deep convection, whether in the form of VHTs or less intense but more widespread convective systems, is crucial to the vorticity budget of tropical cyclones, it is important to determine the mechanisms by which the tropical cyclone environment controls the embedded convection. If vorticity balance is a valid approximation, then perhaps we can assume that the boundary layer convergence predicted by this approximation can tell us the location and intensity of deep convection. However, if vorticity balance does not hold, we must seek other mechanisms by which the convection is controlled.

The THORPEX Pacific Asian Regional Campaign (TPARC) and the associated Tropical Cyclone Structure experiment (TCS08) (Elsberry and Harr, 2008) studied various aspects of western Pacific typhoons in August and September of 2008. Numerous observational tools were focused on the formation and development of typhoons and on their extratropical transitions during this period.

A case of particular interest is the development of Typhoon Nuri (2008) which intensified from a tropical wave to a typhoon in three days. Montgomery et al. (2009) present the synoptic conditions in which the precursor tropical wave developed into a tropical cyclone. They show that the core of the cyclone formed at the critical latitude, i.e., the latitude at which the low-level wind equaled the wave propagation speed. This supports the hypothesis of Dunkerton et al. (2009) that the region of the wave at the critical latitude is favored for development due to the weak wave-relative winds and the lack of import of dry environmental air at this latitude.

We were able to observe tropical cyclone Nuri on four successive days with varying combinations of dropsondes and airborne Doppler radar. On these four days the system was successively a tropical wave (TW), a tropical depression (TD), a tropical storm (TS), and a typhoon (TY). On the whole, the data for the first three days are sufficient to analyze all terms in the vorticity equation (1) through the full depth of the system.

Vorticity budget in Typhoon Nuri

D. J. Raymond and
C. López Carrillo

Title Page

Abstract

Introduction

Conclusions

References

Tables

Figures

⏪

⏩

◀

▶

Back

Close

Full Screen / Esc

Printer-friendly Version

Interactive Discussion



The absence of Doppler radar data limit the analysis on day four. Thus, we captured an unusually complete picture of Nuri's early intensification, shedding significant light on the vorticity dynamics of tropical storm formation. We also observed in a single mission a non-developing tropical wave, designated TCS030. The contrast between this system and the earliest observed stage of Nuri is enlightening.

Section 2 discusses the data sources and analysis methods used in this case study. The vorticity budgets of tropical cyclone Nuri at its various stages and of tropical wave TCS030 are described in Sect. 3. The implications of these results are discussed in Sect. 4 and conclusions are presented in Sect. 5.

2 Data and methods

2.1 TPARC/TCS08

The TPARC/TCS08 field program took place from 1 August through 30 September 2009. Though the main operations center was located at the US Naval Postgraduate School in Monterey, California, aircraft bases were located in Guam, Taiwan, and Japan. Okinawa was sometimes used as an auxiliary aircraft base. Driftsonde balloons capable of deploying dropsondes from stratospheric elevations, were launched from the Island of Hawaii.

The aircraft available to the project were two WC-130J turboprops from the US Air Force Reserve 53rd Weather Reconnaissance Squadron, the US Naval Research Laboratory (NRL) P-3 aircraft (all based in Guam), the Taiwanese DOTSTAR aircraft, a modified Astra business jet operated by the National Taiwan University (Taipei), and the German Dassault Falcon 20-E5 jet operated by the Deutsches Zentrum für Luft- und Raumfahrt (DLR; Atsugi, Japan). All aircraft were capable of deploying dropsondes. In addition, the DLR Falcon carried downward-looking wind, temperature, and water vapor lidars, while the NRL P-3 carried the National Center for Atmospheric Research's ELDORA radar and a Doppler wind lidar.

Vorticity budget in Typhoon Nuri

D. J. Raymond and
C. López Carrillo

Title Page

Abstract

Introduction

Conclusions

References

Tables

Figures



Back

Close

Full Screen / Esc

Printer-friendly Version

Interactive Discussion



2.2 Observations

Table 1 gives information about the four aircraft missions into developing tropical cyclone Nuri and the single mission into TCS030. The aircraft involved in the observations of Nuri were the two WC-130Js and the NRL P-3, all operating out of Guam.

5 Though the P-3 generally operated between elevations of 2.4 km and 3.6 km, it climbed for a short time to 7.3 km during the first mission in order to deploy dropsondes. The WC130J deployed a few dropsondes in Nuri from 9.4 km during the third mission, but had to return to Guam due to mechanical problems. The preferred altitude of operation for the WC130J was 9.4 km, but it descended to 3.0 km when icing or turbulence
10 became a problem at the higher altitude.

Times are given in UTC in this paper. Local time in Guam is UTC+10 h. All on-station times for Nuri and TCS030 flights by the P-3 were in daylight. The Nuri flights launched around 08:00 LT and recovered around 15:00 LT. The TCS030 flight of the P-3 launched at 05:00 LT and recovered near 12:00 LT. The WC-130J generally launched
15 a few hours before the P-3.

The mission of the WC-130Js was to deploy a grid of dropsondes over the disturbance in question from as high an altitude as feasible given the conditions. The main mission of the P-3 was to make Doppler radar measurements of convection using the ELDORA radar. In most cases the strategy was to obtain snapshots of as many convective systems as possible within the cyclone; repeated measurements on convective systems were generally not made, as obtaining a large statistical sample of convection was considered to be more valuable than following the life cycles of a few systems. In addition, the P-3 deployed dropsondes along the flight path and made Doppler wind
20 lidar measurements of the atmospheric boundary layer beneath the aircraft.

The ELDORA radar was configured as shown in Table 2. The unambiguous range of 75 km means that Doppler radar measurements in a 150 km swath were made, centered on the P-3 track, albeit with reduced spatial resolution at the outer limits. Since ELDORA is an X-band radar, attenuation is a significant issue. However, the large
25

Vorticity budget in Typhoon Nuri

D. J. Raymond and
C. López Carrillo

Title Page

Abstract

Introduction

Conclusions

References

Tables

Figures



Back

Close

Full Screen / Esc

Printer-friendly Version

Interactive Discussion



unambiguous velocity of 62 m s^{-1} means that unfolding of radial velocities was not a significant problem with the systems observed in this case study.

The Doppler radar measurements from the P-3 aircraft and dropsondes from the P-3 and the WC130J were used for the first three Nuri missions to produce gridded horizontal and vertical winds satisfying mass continuity using a three-dimensional variational analysis scheme (3-D-VAR). This scheme is described in detail by López Carrillo and Raymond (2010). Only dropsondes deployed during the 4–6 h in which the P-3 was flying in the system were used. The fourth Nuri mission produced only dropsonde data from the WC-130J, and these soundings (deployed from 3 km for operational reasons) were used to produce an analysis with the 3-D-VAR system.

For the first three Nuri missions for which radar data are available and for the single TCS030 mission, the grid resolution is 0.125° in both latitude and longitude (roughly 14 km) and 0.625 km in the vertical. The gridded domain is $5^\circ \times 5^\circ \times 20 \text{ km}$ or $40 \times 40 \times 32$ cells for Nuri missions 2 and 3 and $7^\circ \times 7^\circ \times 20 \text{ km}$ or $56 \times 56 \times 32$ cells for Nuri mission 1 and the TCS030 mission. For the fourth Nuri mission in which only dropsonde data are available, the horizontal grid resolution is also 0.125° with a $4^\circ \times 4^\circ$ domain size, for a grid with $32 \times 32 \times 32$ cells.

Though the 3-D-VAR scheme produces results in the entire domain analyzed, these results are not reliable outside of the region where data exist. The results are therefore masked to include only regions which contain either radar or dropsonde data (or both). At higher altitudes radar data cover less area. Furthermore, the deepest dropsonde soundings begin near roughly 10 km. For this reason, the regions above 12 km are ignored and most results come from observations at 5 km and below. The 3-D-VAR scheme is capable of incorporating high elevation angle radar data. However, radar rays with elevation angles exceeding $\pm 30^\circ$ were not used in the analysis in order to avoid contaminating our results with uncertainties in the estimation of particle terminal velocities. Results obtained with and without this limitation are quite similar, but the high elevation angle data introduce some “cosmetic” artifacts in vertical velocities which we prefer to avoid. A minimum of 200 radar radial velocities are required in each grid cell

Vorticity budget in Typhoon Nuri

D. J. Raymond and
C. López Carrillo

Title Page

Abstract

Introduction

Conclusions

References

Tables

Figures

◀

▶

◀

▶

Back

Close

Full Screen / Esc

Printer-friendly Version

Interactive Discussion



and the condition $a_2 \geq 0.03$ is imposed in order to ensure that only valid dual Doppler results are included (see López and Raymond, 2010). These conditions largely eliminate random outliers in the radar synthesis without significantly limiting radar coverage.

Before applying the 3-D-VAR scheme, radar and dropsonde observations were adjusted to their corresponding positions at a specified reference time using the observed propagation velocity of the disturbance over the measurement period. System positions were estimated from vorticity fields in National Centers for Environmental Prediction Final Analysis (NCEP FNL) data. Both propagation velocities and reference times are listed in Table 1. The low-level circulation centers at the reference time for each mission are also given in this table.

2.3 Vorticity analysis

Once the velocity grid is obtained, all components of the vorticity are computed using centered differences. The first two terms on the right side of (1) are then computed from the vorticity and the velocity. The advection and stretching components of the first term are also computed separately.

In order to compute the third term, the surface wind stress needs to be calculated and an assumption has to be made about the depth over which the stress is distributed. The surface stress τ is computed from a bulk flux formula

$$\tau = -\rho_{BL} C_D |\mathbf{U}_{BL}| \mathbf{U}_{BL}, \quad (4)$$

where a subscripted BL indicates a boundary layer value, with ρ indicating air density and \mathbf{U} indicating horizontal wind. Since Doppler radar observations close to the surface are problematic due to problems with sea clutter, \mathbf{U}_{BL} is derived primarily from radar (and dropsonde) winds at the first radar level above the surface at $z=0.625$ km.

Results from the CBLAST (Coupled Boundary Layer Air–Sea Transfer) experiment (Fig. 5 of Black et al., 2007) suggest an estimate for the drag coefficient

$$C_D \approx (1 + 0.028|\mathbf{U}_{BL}|) \times 10^{-3} \quad (5)$$

Vorticity budget in Typhoon Nuri

D. J. Raymond and
C. López Carrillo

Title Page

Abstract

Introduction

Conclusions

References

Tables

Figures

◀

▶

◀

▶

Back

Close

Full Screen / Esc

Printer-friendly Version

Interactive Discussion



thought to be valid up to approximately 30 m s^{-1} . Since CBLAST results are for 10 m winds, our use of winds near 625 m results in a slight overestimate for the surface stress.

The specific frictional force F is postulated to take the form

$$\rho F \approx \tau \exp(-z/z_s)/z_s, \quad (6)$$

where a scale height of $z_s = 1.25 \text{ km}$ is chosen represent the average depth of the planetary boundary layer (PBL) in tropical regions. A weakness of this analysis is that we do not know the vertical distribution of F . However, the postulated form is consistent with the idea that surface friction is mixed through the PBL via turbulent eddies. Given the uncertainties noted above, F is probably known to within only a factor of two. However, this accuracy is sufficient to draw some significant conclusions, as noted below.

With F roughly known, the third term on the right side of (1) is estimated. Integrating this equation over a horizontal area A and applying Gauss's law, we obtain the tendency of the absolute circulation around the area A ,

$$\frac{d\Gamma}{dt} = -\oint v_n \zeta_z dl + \oint \zeta_n v_z dl + \oint F_t dl, \quad (7)$$

where the line integrals are taken to be in the counterclockwise direction over the periphery of A , v_n and ζ_n are the horizontal outward normal components of the velocity and vorticity, and F_t is the component of F tangential to the periphery of A in the direction of the integration. Thus, the circulation around the area A depends only on what is happening on the periphery of A and not in the interior. The first term on the right is the spinup tendency due to the convergence of absolute vorticity, the second expresses the effect of vortex tilting on the periphery of A , and the third is the spindown tendency due to friction.

The terms on the right side of (7) may be computed directly, or by area integrating the right side of (1). We choose the latter approach as it is computationally simpler. In addition, by expressing the horizontal velocity v_h as relative to the motion of a propa-

Vorticity budget in Typhoon Nuri

D. J. Raymond and
C. López Carrillo

Title Page

Abstract

Introduction

Conclusions

References

Tables

Figures

◀

▶

◀

▶

Back

Close

Full Screen / Esc

Printer-friendly Version

Interactive Discussion



Discussion Paper | Discussion Paper | Discussion Paper | Discussion Paper | Discussion Paper

gating system, the circulation tendency around the moving system can be computed using (7).

We adopt this approach in the analysis of the Nuri and TCS030 missions. The motions of the propagating systems are estimated from a combination of FNL vorticity centers every 6 h and observed low-level circulation centers obtained from our aircraft observations. The estimates are somewhat subjective, but our results are not sensitive to the likely errors in these estimates, which are of order $\pm 1 \text{ m s}^{-1}$. Our estimates of system-relative velocity are shown in Table 1.

3 Results

In this section we document the overall development of Nuri and of the tropical wave TCS030. We then examine the vorticity structure of these systems and finally analyze the vorticity dynamics of intensification.

3.1 Overview of development

Figure 1 shows the locations of tropical cyclone Nuri determined from FNL 850 hPa vorticity patterns as well as low-level circulation centers from our observational analysis, along with the Reynolds (Reynolds and Marsico, 1993) sea surface temperature (SST) distribution for the period of Nuri's intensification. Previous to the typhoon stage, Nuri passed over SSTs of approximately 30°C . It later encountered decreasing SSTs. The FNL positions are obtained from subjective estimates of the vorticity center. As the scatter in successive position estimates shows, this procedure is not very precise in the tropical wave stage. It also appears to lead to a systematic southward displacement of the estimated position of Nuri during this phase, compared to our observations of the low-level circulation center.

Figure 2 shows a time series of the distribution in satellite infrared brightness temperature in a $5^\circ \times 5^\circ$ square centered on Nuri as it intensified and moved to the west. The

Vorticity budget in Typhoon Nuri

D. J. Raymond and
C. López Carrillo

Title Page

Abstract

Introduction

Conclusions

References

Tables

Figures

◀

▶

◀

▶

Back

Close

Full Screen / Esc

Printer-friendly Version

Interactive Discussion



input for this figure is a series of Japanese MTSAT geosynchronous satellite infrared images interpolated to a longitude-latitude grid with a resolution of $0.2^\circ \times 0.2^\circ$. A pronounced diurnal cycle is seen, with coldest cloud tops occurring near 18:00 UTC. This diurnal cycle diminishes in amplitude as the storm intensifies and produces a more extensive region of high overcast. Note that the aircraft missions took place during periods of warming cloud tops. Operational constraints prevented us from exploring the diurnal cycle with the aircraft.

Figure 3 shows the SST at the time TCS030 was observed and its location at this time. SSTs were in excess of 30°C and the system was moving toward even warmer water. In spite of these favorable conditions, TCS030 did not develop. Instead it fluctuated in intensity and finally made landfall in the southern Philippines as a tropical wave. The white star in Fig. 3 was located near the most intense convection observed in TCS030 since no low-level circulation center was obvious. This estimate was displaced well to the northeast of the position estimate based on FNL 850 hPa vorticity.

3.2 Vorticity structure

Figures 4–6 show the storm-relative winds and absolute vorticity at 1.2 km and 5 km for the first three missions into tropical cyclone Nuri. The track of the P-3 aircraft and locations of usable dropsondes are shown in the left-hand panels. Reflectivities greater than 25 dBZ at 5 km are shown as gray-scale insets in the right-hand panels.

As storm-relative winds are used, the circulation centers in both panels are physically significant since the associated streamlines are close to being parcel trajectories. These circulation centers are also important thermodynamically, as they are protected from the injection of dry air from outside the system (Dunkerton et al., 2009) The 1.2 km circulation centers are listed in Table 1 and shown Fig. 1.

The low-level circulation center is somewhat ill-defined in the case of Nuri 1, though it is plausibly located at the white star in Fig. 4. The low-level vorticity in Nuri 1 shows a northwest-southeast band to the northeast of the assumed center (Fig. 4) and an otherwise random pattern of vorticity fluctuations. The band bounds the southern limit

Vorticity budget in Typhoon Nuri

D. J. Raymond and
C. López Carrillo

Title Page

Abstract

Introduction

Conclusions

References

Tables

Figures

◀

▶

◀

▶

Back

Close

Full Screen / Esc

Printer-friendly Version

Interactive Discussion



of the strong cyclonic flow on the north side of the system. At 5 km, the pattern is quite different, with the strongest vorticity on the east and southeast sides of the disturbance. Visual observation from the P-3 indicated that this region of vorticity aloft coincided with a large stratiform rain area. This is in contrast with the western part of the disturbance, which exhibited a much more convective structure. The elongated center of the system-relative circulation at 5 km is in the form of a northeast-southwest band displaced $\approx 3^\circ$ to the southeast of the low-level center. The southwestern end of this band is close to the position inferred from FNL 850 hPa vorticity. Maximum relative winds are near 10 m s^{-1} at both levels.

The strength of vorticity perturbations has intensified at both 1.2 km and 5 km in Nuri 2 (see Fig. 5), though there is still little system-wide organization at 1.2 km. The 1.2 km circulation center is located at the northwest corner of the observed region in this case and the circulation center at 5 km is displaced $\approx 2^\circ$ to the south of the low-level center. At 5 km there is a rather strong north-south band of vorticity located roughly between the low and mid-level circulation centers. The overall circulation is slightly stronger than that seen in Nuri 1. Maximum relative winds are near 15 m s^{-1} , with slightly stronger winds occurring at 5 km.

Figure 6 shows that the circulation pattern has changed drastically for Nuri 3, with a strong central vorticity maximum at 1.2 km and a spiral band of vorticity linked to the central maximum. A nearly co-located maximum in vorticity exists at 5 km. The maximum winds are about 20 m s^{-1} at both levels, with the largest values occurring near the central vorticity maximum.

Figure 7 shows the vorticity and storm-relative winds for mission 4. No radar reflectivities are available due to the absence of the P-3 in this mission. The circulation center is clearly defined at this stage. Due to the lack of observations between the legs of the “X” pattern flown by the WC-130J, the analyzed winds in the outer regions are somewhat questionable. However, with the concentration of observations near the circulation center, the winds are likely to be more reliable there. Maximum winds are near 40 m s^{-1} and the near-core circulation is highly symmetric.

Vorticity budget in Typhoon Nuri

D. J. Raymond and
C. López Carrillo

[Title Page](#)[Abstract](#)[Introduction](#)[Conclusions](#)[References](#)[Tables](#)[Figures](#)[⏪](#)[⏩](#)[◀](#)[▶](#)[Back](#)[Close](#)[Full Screen / Esc](#)[Printer-friendly Version](#)[Interactive Discussion](#)

Vorticity budget in Typhoon Nuri

D. J. Raymond and
C. López Carrillo

Title Page

Abstract

Introduction

Conclusions

References

Tables

Figures

◀

▶

◀

▶

Back

Close

Full Screen / Esc

Printer-friendly Version

Interactive Discussion



The circulation in the case of TCS030 (Fig. 8) is very weak, with maximum system-relative winds less than 10 m s^{-1} . To the extent that a circulation can be inferred at 1.2 km, it is centered at the far northeast corner of the observed region. The system-relative flow through the system at low levels is from the west. Though there is a region of moderately strong 5 km vorticity near the northeast corner, the flow at this level does not suggest a closed circulation even in storm-relative coordinates. In general, vorticities are less than they are in Nuri 1.

Figure 9 shows histograms of the relative frequency of occurrence of vorticity values at 1.2 km elevation seen in Figs. 4–6 and 8. (Results from Fig. 7 are not included as fine resolution radar data were not available in this case.) As Nuri intensified, larger values of vorticity developed as expected. However, the overall distribution broadened as well, with more negative values also occurring. Negative absolute vorticity values are likely produced by the tilting term in the vorticity equation; the only other possible mechanism would be convergence of pre-existing negative vorticity, which could in principle occur, but seems less likely. Increased convective activity in shear, which promotes tilting, is probably how this happens. The strong vorticities in the central maximum seen in Fig. 6 are highly limited in areal coverage and appear in the extreme tail of the Nuri 3 distribution. Thus, the central maximum contributes to only a small part of the overall circulation around the system in the tropical storm stage of Nuri. The distribution of vorticity in the tropical wave TCS030 is somewhat similar to that in the tropical wave stage of Nuri, but with more negative and fewer positive values of absolute vorticity.

Figure 10 shows vertical profiles of wind for the Nuri missions and the TCS030 mission. All but the Nuri 3 profiles were obtained from averaging analyzed winds from the 3-D-VAR scheme over the full domains of Figs. 4, 5, 7, and 8. There is likely to be some contamination of the environmental flow with storm generated winds in this case, but by averaging over the entire domain, which is at least somewhat centered on the disturbance, much of this contamination should average out. For Nuri 3, a smaller but symmetric region consisting of a one-degree square centered at $(132.8^\circ, 16.1^\circ)$ was averaged rather than the entire domain, since the asymmetry of the full observed

region relative to the core is likely to increase greatly the contamination of the environmental flow with cyclone-generated winds. However, this method of reducing the cyclone contribution is sensitive to small asymmetries in the cyclone flow, which reduce the representativeness of the calculated sounding. The Nuri 4 sounding is also likely to be less representative for the same reasons.

This figure shows moderately strong shears, with easterly to northeasterly shear of $\approx 7 \text{ m s}^{-1}$ between the surface and 6 km. This shear was strong enough in the real time forecast for TPARC/TCS-08 forecasters to discount the possibility that Nuri would intensify; the initial mission was therefore undertaken as a probable “null” case! The relative wind profile in TCS030 differed little in essential characteristics from that seen in Nuri 1 with the exception that strong northerly system-relative flow existed at middle and upper levels.

3.3 Circulation dynamics

As noted in Sect. 2, the advective (Z_1 in (1)) and non-advective fluxes ($Z_2 + Z_f$) of the vertical component of absolute vorticity are estimated from the velocity fields. Figures 11–14 show the total vorticity flux and the vorticity tendency due to vertical stretching for Nuri 1–3 and TCS030 in the PBL and at 5 km. The stretching tendency $-\zeta_z \nabla_h \cdot \mathbf{v}_h$ is shown rather than the total tendency because stretching is the main mechanism by which parcel values of vorticity are increased, at least in regions of small tilting tendency. The vorticity advective tendency $-\mathbf{v}_h \cdot \nabla_h \zeta_z$ exhibits complex patterns which are irrelevant to the parcel increase in vorticity, though of course its contributions are needed to compute the overall circulation tendency given by (7). Also shown is the total vorticity flux. The vorticity flux (but not the stretching tendency) has been low-pass filtered with a filter length of 0.5° to improve the clarity of the overall vorticity flow patterns. Mostly the vorticity flux reflects the horizontal velocity field, demonstrating the large magnitude of the advective part of the vorticity flux relative to the non-advective part.

Vorticity budget in Typhoon Nuri

D. J. Raymond and
C. López Carrillo

Title Page

Abstract

Introduction

Conclusions

References

Tables

Figures

◀

▶

◀

▶

Back

Close

Full Screen / Esc

Printer-friendly Version

Interactive Discussion



Vorticity budget in Typhoon Nuri

D. J. Raymond and
C. López Carrillo

Title Page

Abstract

Introduction

Conclusions

References

Tables

Figures

◀

▶

◀

▶

Back

Close

Full Screen / Esc

Printer-friendly Version

Interactive Discussion



The stretching tendency of vorticity indicates regions of mass convergence, so maxima in this quantity indicate regions of convection with significant convergence in the boundary layer. Comparison of stretching maxima in the PBL with regions of strong 5 km reflectivity in the right panels of Figs. 4–6 and 8 shows moderately good, but not perfect agreement in this respect. Notable examples exhibiting strong correlations in this regard include the convection near (145.8° E, 14.2° N) in Nuri 1, (140.2° E, 14.4° N) in Nuri 2, and (133.0° E, 16.0° N) in Nuri 3. The large area of convection centered near (141.5° E, 14.3° N) in TCS030 lacks PBL stretching, suggesting weak vertical mass flux at low levels in this case. An examination of the mass flux profile in this region (not shown) verifies this conclusion.

As Nuri intensifies, the regions of stretching become fewer and more intense, culminating in a single strong central vortex in Nuri 3. This suggests a transformation from scattered ordinary convection to a more limited number of strong convective systems reminiscent of VHTs, which in turn give way to the cyclone eyewall.

Closed circulations of vorticity flux in Nuri 1–3, as seen in Figs. 11–13, show that regions of strong vorticity created by stretching are not exported from Nuri during its growing stage. The centers of these vorticity circulations are near, but not necessarily colocated with the centers of mass circulations. This difference in location is due to a combination of non-advective fluxes, i.e., tilting and frictional fluxes represented by the second and third terms on the right side of (1). The pattern of vorticity transport in TCS030 is not closed, allowing vorticity maxima in the PBL to be exported from this system.

The strongest tendencies at 5 km are greater than PBL tendencies in Nuri 1, Nuri 2, and in TCS030. As in the PBL, the vorticity flux exhibits closed circulations in Nuri 1–3 (centers indicated by the white circles), but not in TCS030. However, as Figs. 11 and 12 show, the centers of the 5 km vorticity circulations can be displaced by as much as 3° from those in the PBL. This displacement decreases as Nuri intensifies.

Figures 15–19 show vertical profiles of absolute circulation around the observed regions in Figs. 4–6 and 8 and vertical mass fluxes integrated over these regions. In

5 addition, the vertical profiles of the various components of circulation tendency are shown. By hypothesis, the friction tendency is concentrated primarily in the PBL. The domain sizes are different for each case. However, all curves are normalized by the magnitude of the planetary circulation (the area integral of the Coriolis parameter) to facilitate the comparison between profiles in the different cases.

10 Figure 15 shows profiles for Nuri 1. Curiously, the maximum circulation in this tropical wave case occurs in a nearly uniform layer from the surface up to 4 km with a value of roughly twice the planetary circulation. The circulation decreases monotonically above this level. The vertical mass flux maximizes at high levels, near 10 km elevation, and the z derivative of the circulation with height is very small in the PBL. Thus, boundary layer convergence due to convection is very small and the circulation tendency due to vorticity convergence near the surface is correspondingly small. The frictional spindown tendency exceeds vorticity convergence below 1 km. Vorticity convergence increases up to the mid-troposphere and then decreases. Above this level tilting makes a significant positive contribution to the circulation tendency.

15 Nuri 2 (Fig. 16) exhibits a very different pattern, with the vorticity convergence term greatly exceeding frictional spindown in the PBL. This is related to the strongly increasing vertical mass flux with height in the PBL, which implies strong inflow in this layer. The mass flux maximizes near an elevation of 5 km, which is significantly lower than in Nuri 1. The contribution of tilting is weak at all levels. The surface circulation is still only about twice the planetary circulation, but the maximum circulation has increased to three times the planetary circulation near 5 km.

20 Figure 17 shows that for Nuri 3 the normalized mean circulation has increased at all levels in comparison to Nuri 2. The elevation of maximum vertical mass flux has increased to near 6 km and the z derivative of mass flux with height in the PBL is less than for Nuri 2. Tilting contributes negatively to the circulation tendency in the lower troposphere and positively in the upper troposphere. However, this may be an artifact of the location of the circulation center near the edge of the observed region.

Vorticity budget in Typhoon Nuri

D. J. Raymond and
C. López Carrillo

[Title Page](#)[Abstract](#)[Introduction](#)[Conclusions](#)[References](#)[Tables](#)[Figures](#)[◀](#)[▶](#)[◀](#)[▶](#)[Back](#)[Close](#)[Full Screen / Esc](#)[Printer-friendly Version](#)[Interactive Discussion](#)

Vorticity budget in Typhoon Nuri

D. J. Raymond and
C. López Carrillo

Title Page

Abstract

Introduction

Conclusions

References

Tables

Figures

◀

▶

◀

▶

Back

Close

Full Screen / Esc

Printer-friendly Version

Interactive Discussion



The circulation tendency due to vorticity convergence is actually negative in the PBL, but this is due to the apparent suppression of stretching away from the central vorticity maximum. The circulation tendency in the PBL for a 2° -square box centered on the core (Fig. 18) is positive. Comparison of Figs. 17 and 18 also shows that the region within the 2° box is responsible for 2/3 of the mass flux and circulation and nearly 100% of the circulation at the surface. These results reflect a significant reduction in scale of the dynamically active part of the tropical cyclone as it intensifies.

In the TCS030 case (Fig. 19) the circulation is almost non-existent and the vertical mass flux is very weak. Curiously, the mass flux profile has a double maximum, with peak fluxes near 2 km and 8 km. Even though the z derivative of mass flux in the PBL is quite large in spite of the weak overall profile, the vorticity convergence tendency in the PBL (and at all levels) is negative due to the export of vorticity. This export is related to the lack of a closed vorticity flux circulation in the PBL, as shown in Fig. 14. The circulation tendency due to tilting is positive in the upper troposphere. However, as in Nuri 3, this is apparently the consequence of the proximity of strong convection at 144.5° E, 14° N to the boundary of the observed region.

4 Discussion

The formation of Typhoon Nuri over a three day period was documented by aircraft missions on four successive days. During this period the cyclone evolved from a tropical wave to a tropical depression, a tropical storm, and finally to a full-fledged typhoon. This rapid intensification occurred in an environment of significant easterly and north-easterly shear (Fig. 10). Intensification began near the island of Guam. The storm followed a track toward the west during this period and Nuri was just to the east of the Philippines during the last mission (see Fig. 1).

Figures 4–7 demonstrate that Nuri had broadly distributed vorticity anomalies well in excess of the planetary vorticity at all stages (at least for Nuri 1–3 in which we had radar data). This is quantified in Fig. 9 and is most likely due to the concentrating

effects of mesoscale convective systems, which leave behind residual vortices after they decay (Hendricks et al., 2004; Montgomery et al., 2006). As Nuri evolved, the vorticity distribution broadened, acquiring slightly more positive mean values, and developing a long positive tail representing the central core of vorticity. The broadening with time suggests the development of more intense convective systems in a regime of increasing background vorticity. The increase in negative vorticity values suggests a significant role for the tilting term in the vorticity equation on the mesoscale, though Figs. 15–17 demonstrate that tilting played a minor role on the system-wide scale.

In Nuri 1 and Nuri 2, the circulation centers in the PBL and at 5 km are displaced from each other by 2° – 3° . Comparison of Figs. 4 and 5 with the shears shown in Fig. 10 shows that the displacement of the 5 km circulation center relative to the PBL center is approximately 90° to the left of the shear vector between the PBL and 5 km. Thus, in the case of Nuri 1, the shear is from the northeast and the 5 km circulation is southeast of the PBL circulation. For Nuri 2 the shear is more easterly and the corresponding circulation center displacement is to the south.

Figure 20 explains why the system-relative circulation centers are displaced from each other. At each level the total wind is assumed to be the vector sum of the system-relative ambient wind and the induced circulation associated with the wave-scale region of positive relative vorticity, which is assumed to encompass the closed circulations at both levels. The circulation center at each level occurs where the vector sum of these winds is zero. The displacement between these circulation centers is due to the difference in the ambient wind between the two levels, with the displacement being normal to the shear vector.

Associated with these circulation centers are regions exhibiting closed cyclonic circulations. Air (and vorticity) at each level inside the bounding closed streamline remains within the system and is protected from incursions by environmental air as postulated by Dunkerton et al. (2009) and Montgomery et al. (2009). The area where these regions overlap is protected from environmental incursions through the full column depth between the PBL and 5 km. It is thus likely to be the area in which the core of the de-

Vorticity budget in Typhoon Nuri

D. J. Raymond and
C. López Carrillo

[Title Page](#)[Abstract](#)[Introduction](#)[Conclusions](#)[References](#)[Tables](#)[Figures](#)[◀](#)[▶](#)[◀](#)[▶](#)[Back](#)[Close](#)[Full Screen / Esc](#)[Printer-friendly Version](#)[Interactive Discussion](#)

veloping tropical cyclone spins up. In Nuri 1 this region contained the strongest deep convection. In Nuri 2 the most significant vorticity at 5 km was also found in this region, suggesting a history of strong convection there.

Note that this explanation for the displacement of the circulation center with height differs from explanations based on adiabatic vortex dynamics, such as those of Jones (1995, 2000a,b) which are based on the interaction between potential vorticity patterns at different elevations. Our explanation depends on the existence (and continuous production) of background vorticity associated with vortex stretching in deep convection over the region of the wave.

Nuri transformed from a pattern of scattered mesoscale vortices to a highly organized system with a strong central concentration of vorticity between mission 2 and mission 3. However, this transformation was not sudden; examination of Figs. 11–13 shows that the number of regions of vortex stretching decreased as Nuri evolved and the strength of the stretching increased. This suggests the development of fewer but stronger convective systems (VHTs?) as Nuri intensified, culminating in a single core system which developed into the eyewall.

As it evolved, Nuri's convection exhibited a variety of vertical mass flux profiles. In the tropical wave stage (Nuri 1) the average mass flux peaked at a high elevation, resulting in a deep but weak inflow. As a result, the circulation was decaying in the PBL, but increasing in the free troposphere. This is reflected in the greatly increased mid-level circulation seen in Nuri 2. While a tropical depression (Nuri 2) the mass flux increased rapidly with height below 4 km, resulting in an intense inflow in the PBL. This inflow was responsible for the strong positive circulation tendency associated with vorticity convergence. In the tropical storm stage (Nuri 3) the PBL inflow was less strong overall, resulting in a net spindown tendency in the PBL. However, as Fig. 13 shows, the spinup tendency near the circulation center was intense, suggesting that a decrease in scale occurred during the tropical storm stage. Due to the lack of Doppler radar data in Nuri 4, we are unable to say much about the vertical mass flux profile in the typhoon stage.

Vorticity budget in Typhoon Nuri

D. J. Raymond and
C. López Carrillo

Title Page

Abstract

Introduction

Conclusions

References

Tables

Figures

◀

▶

◀

▶

Back

Close

Full Screen / Esc

Printer-friendly Version

Interactive Discussion



Vorticity budget in Typhoon Nuri

D. J. Raymond and
C. López Carrillo

Title Page

Abstract

Introduction

Conclusions

References

Tables

Figures

◀

▶

◀

▶

Back

Close

Full Screen / Esc

Printer-friendly Version

Interactive Discussion



Superficially, the pre-Nuri tropical wave observed during Nuri 1 was similar to the wave seen in TCS030. Both cases appeared as tropical waves in large-scale analyses and both had similar values of shear. However, the TCS030 system did not exhibit closed circulations at the two levels studied, even in system-relative coordinates. This probably explains why TCS030 did not spin up. Intensification of a tropical cyclone in shear thus takes on the character of a “chicken and egg” problem; in order for spinup to occur, there must be a pre-existing broad distribution of relative vorticity through the low to middle troposphere. However, creation of this vorticity anomaly is difficult without protection against ventilation by the environment. Nuri was lucky enough to have developed this vorticity pattern by the time we began our observations, whereas TCS030 was not so favored.

A particularly interesting aspect of Nuri’s evolution is that vorticity balance in the PBL was far from satisfied. In Nuri 1 and Nuri 3 (full observed region) the frictional spin-down tendencies slightly exceeded the spinup tendencies due to vorticity convergence. In Nuri 2 spinup due to vorticity convergence far exceeded frictional spindown. Only in the restricted region encompassing the core of Nuri 3 was approximate vorticity balance observed (see Fig. 18). Uncertainties in the vertical distribution of surface stress are insufficient to explain this discrepancy, particularly for Nuri 2. Thus, the Ekman pumping hypothesis, in which low-level convergence implied by Ekman (or vorticity) balance is assumed to control deep convection, appears problematic in this case, at least in the phases preceding tropical storm strength. The effects of tilting are generally insufficient to change these qualitative results, at least at low levels.

5 Conclusions

Our analyses of Typhoon Nuri and tropical wave TCS030 support the following conclusions:

1. Nuri spun up rapidly from a tropical wave to a typhoon in spite of significant environmental shear. TCS030 was subject to similar shear and did not spin up.

**Vorticity budget in
Typhoon Nuri**D. J. Raymond and
C. López Carrillo[Title Page](#)[Abstract](#)[Introduction](#)[Conclusions](#)[References](#)[Tables](#)[Figures](#)[◀](#)[▶](#)[◀](#)[▶](#)[Back](#)[Close](#)[Full Screen / Esc](#)[Printer-friendly Version](#)[Interactive Discussion](#)

This difference in behavior was probably related to the existence of a pre-existing tropical-depression-scale circulation in Nuri at the tropical wave stage and its absence in TCS030.

2. The displacement of the center of the Nuri circulation with height is explained as the result of the interaction of a large region of positive relative vorticity with shear. This displacement, though of order 2° – 3° between the surface and 5 km in the wave and tropical depression stages, was still small enough for a column protected from environmental incursions to exist through this elevation range.
3. As Nuri intensified, regions of convective vortex stretching became fewer and more intense, culminating in the formation of a strong central vortex.
4. The tilting term in the vorticity equation was relatively small on a system-wide basis in the lower troposphere even given the presence of strong wind shear. However, it was more significant on the mesoscale, and was likely responsible for the large negative absolute vorticities seen on small scales.
5. Vorticity balance in the PBL did not exist consistently in our observations, even when integrated over a large area. In particular, during the intensification from tropical depression to tropical storm, the positive circulation tendency due to vorticity convergence far exceeded the spindown tendency of surface friction.

This work complements the larger-scale view of Nuri presented by Montgomery et al. (2009).

Acknowledgements. We thank Mike Herman for the FNL results; Jorge Cisneros for the storm propagation speeds; Chris Velden and Dave Stettner of SSEC for the MTSAT data; crews of the NRL P-3 and the Air Force Reserve WC-130Js for their excellent work; NCAR EOL crew for their dedication, especially in rebuilding ELDORA in the two weeks before the project and in dealing with severe dropsonde problems; and Pat Harr for his exemplary leadership. Quality control of dropsondes by EOL contributed to the fidelity of our analysis. We also thank Kerry Emanuel and Sharon Sessions for useful comments on this manuscript and Mike Montgomery

for many interesting discussions. This work was supported by grants N000140810241 from the Office of Naval Research and ATM0638801 from the US National Science Foundation. C. López was partially supported by Inter-American Institute for Global Change Research grant CRN-2048.

5 References

- Bister, M. and Emanuel, K. A.: The genesis of hurricane Guillermo: TEXMEX analyses and a modeling study, *Mon. Weather Rev.*, 125, 2662–2682, 1997. 16592
- Black, P. G., D’asaro, E. A., Drennan, W. M., French, J. R., Niiler, P. P., Sanford, T. B., Terrill, E. J., Walsh, E. J., and Zhang, J. A.: Air-sea exchange in hurricanes: synthesis of observations from the coupled boundary layer air-sea transfer experiment, *Bull. Am. Meteor. Soc.*, 88, 357–374, 2007. 16598
- Davis, C. A.: Piecewise potential vorticity inversion, *J. Atmos. Sci.*, 49, 1397–1411, 1992. 16592
- Dunkerton, T. J., Montgomery, M. T., and Wang, Z.: Tropical cyclogenesis in a tropical wave critical layer: easterly waves, *Atmos. Chem. Phys.*, 9, 5587–5646, doi:10.5194/acp-9-5587-2009, 2009. 16594, 16601, 16608
- Elsberry, R. L. and Harr, P. A.: Tropical cyclone structure (TCS08) field experiment science basis, observational platforms, and strategy, *Asia-Pacific J. Atmos. Sci.*, 44, 209–231, 2008. 16594
- Emanuel, K. A.: An air-sea interaction theory for tropical cyclones. Part I: Steady state maintenance, *J. Atmos. Sci.*, 43, 585–604, 1986. 16592
- Haynes, P. H. and McIntyre, M. E.: On the evolution of vorticity and potential vorticity in the presence of diabatic heating and frictional or other forces, *J. Atmos. Sci.*, 44, 828–841, 1987. 16590
- Hendricks, E. A., Montgomery, M. T., and Davis, C. A.: The role of vortical hot towers in the formation of tropical cyclone Diana (1984), *J. Atmos. Sci.*, 61, 1209–1232, 2004. 16593, 16608
- Jones, S. C.: The evolution of vortices in vertical shear, I: Initially barotropic vortices, *Quart. J. Roy. Meteor. Soc.*, 121, 821–851, 1995. 16609
- Jones, S. C.: The evolution of vortices in vertical shear, II: Large-scale asymmetries, *Quart. J. Roy. Meteor. Soc.*, 126, 3137–3159, 2000a. 16609

Vorticity budget in Typhoon Nuri

D. J. Raymond and
C. López Carrillo

Title Page

Abstract

Introduction

Conclusions

References

Tables

Figures

◀

▶

◀

▶

Back

Close

Full Screen / Esc

Printer-friendly Version

Interactive Discussion



**Vorticity budget in
Typhoon Nuri**D. J. Raymond and
C. López Carrillo

Title Page

Abstract

Introduction

Conclusions

References

Tables

Figures

◀

▶

◀

▶

Back

Close

Full Screen / Esc

Printer-friendly Version

Interactive Discussion



- Jones, S. C.: The evolution of vortices in vertical shear, III: Baroclinic vortices, *Quart. J. Roy. Meteor. Soc.*, 126, 3161–3185, 2000b. 16609
- López Carrillo, C. and Raymond, D. J.: A three-dimensional variational scheme for analyzing Doppler radar and dropsonde data, in preparation, 2010. 16597
- 5 Montgomery, M. T., Nicholls, M. E., Cram, T. A., and Saunders, A. B.: A vortical hot tower route to tropical cyclogenesis, *J. Atmos. Sci.*, 63, 355–386, 2006. 16593, 16608
- Montgomery, M. T., Lussier III, L. L., Moore, R. W., and Wang, Z.: The genesis of Typhoon Nuri as observed during the Tropical Cyclone Structure 2008 (TCS-08) field experiment – Part 1: The role of the easterly wave critical layer, *Atmos. Chem. Phys. Discuss.*, 9, 19159–19203, doi:10.5194/acpd-9-19159-2009, 2009. 16594, 16608, 16611
- 10 Ooyama, K.: Numerical simulation of the life cycle of tropical cyclones, *J. Atmos. Sci.*, 26, 3–40, 1969. 16591
- Raymond, D. J., López-Carrillo, C., and López Cavazos, L.: Case-studies of developing East Pacific easterly waves, *Quart. J. Roy. Meteor. Soc.*, 124, 2005–2034, 1998. 16592, 16593
- 15 Reynolds, R. W. and Marsico, D. C.: An improved real-time global sea surface temperature analysis, *J. Climate*, 6, 114–119, 1993. 16600
- Ritchie, E. A. and Holland, G. J.: Scale interactions during the formation of Typhoon Irving, *Mon. Weather Rev.*, 125, 1377–1396, 1997. 16592
- Smith, R. K. and Montgomery, M. T.: Balanced boundary layers used in hurricane models, *Quart. J. Roy. Meteor. Soc.*, 134, 1385–1395, 2008. 16591
- 20 Zehnder, J. A.: A comparison of convergence- and surface-flux-based convective parameterizations with applications to tropical cyclogenesis, *J. Atmos. Sci.*, 58, 283–301, 2001. 16592

Vorticity budget in Typhoon Nuri

D. J. Raymond and
C. López Carrillo

Table 1. Information about the four flights into Nuri (15–19 August) and one into TCS030 (1–2 September). The second and third columns give the operation altitude of the two aircraft. The fourth column specifies the reference time to which all observations are reduced, given in units of kiloseconds since the UTC beginning of the first date listed in column one. Thus, reference times exceeding 86.4 ks actually occur on the following UTC day. The fifth and sixth columns give the location of the low-level circulation center of the system at the reference time and the eastward and northward components of the observed propagation speed of the system.

Date	P3	WC130J	Ref time	Ref location	Storm velocity
15–16 Aug	2.4 km	9.4 km	93.0 ks	(145.5° E, 15.5° N)	(−4.9, 0.0) m s ^{−1}
16–17 Aug	2.4 km	9.4 km	86.0 ks	(140.0° E, 16.7° N)	(−8.7, 0.0) m s ^{−1}
17–18 Aug	3.6 km	–	90.0 ks	(132.7° E, 16.5° N)	(−8.7, 0.6) m s ^{−1}
18–19 Aug	–	3.0 km	83.0 ks	(127.1° E, 17.1° N)	(−6.8, 1.9) m s ^{−1}
1–2 Sep	2.4 km	9.4 km	76.0 ks	(145.0° E, 14.5° N)	(−6.3, 0.6) m s ^{−1}

[Title Page](#)
[Abstract](#)
[Introduction](#)
[Conclusions](#)
[References](#)
[Tables](#)
[Figures](#)
[Back](#)
[Close](#)
[Full Screen / Esc](#)
[Printer-friendly Version](#)
[Interactive Discussion](#)


Vorticity budget in Typhoon Nuri

D. J. Raymond and
C. López Carrillo

Table 2. Characteristics of the ELDORA radar during TPARC/TCS08.

Radar characteristic	Value
Wavelength	3.2 cm
Beamwidth ($H \times V$)	$1.8^\circ \times 2.0^\circ$
Antenna gain	39.2 dB
Beam tilt angle	$+15.6^\circ$ fore; -16.5° aft
Antenna rotation rate	$\approx 78^\circ \text{ s}^{-1}$
Peak transmitted power	40 kW
Pulse repetition frequency	1600/2000 Hz
Minimum detectable signal at 10 km	-12 dBZ
Unambiguous range	75 km
Unambiguous velocity (dual PRT)	$\pm 62 \text{ m s}^{-1}$
Number of frequencies	3
Total cell length	150 m
Along track sweep spacing	$\approx 500 \text{ m}$

Title Page

Abstract

Introduction

Conclusions

References

Tables

Figures

◀

▶

◀

▶

Back

Close

Full Screen / Esc

Printer-friendly Version

Interactive Discussion



**Vorticity budget in
Typhoon Nuri**D. J. Raymond and
C. López Carrillo

Title Page

Abstract

Introduction

Conclusions

References

Tables

Figures

◀

▶

◀

▶

Back

Close

Full Screen / Esc

Printer-friendly Version

Interactive Discussion

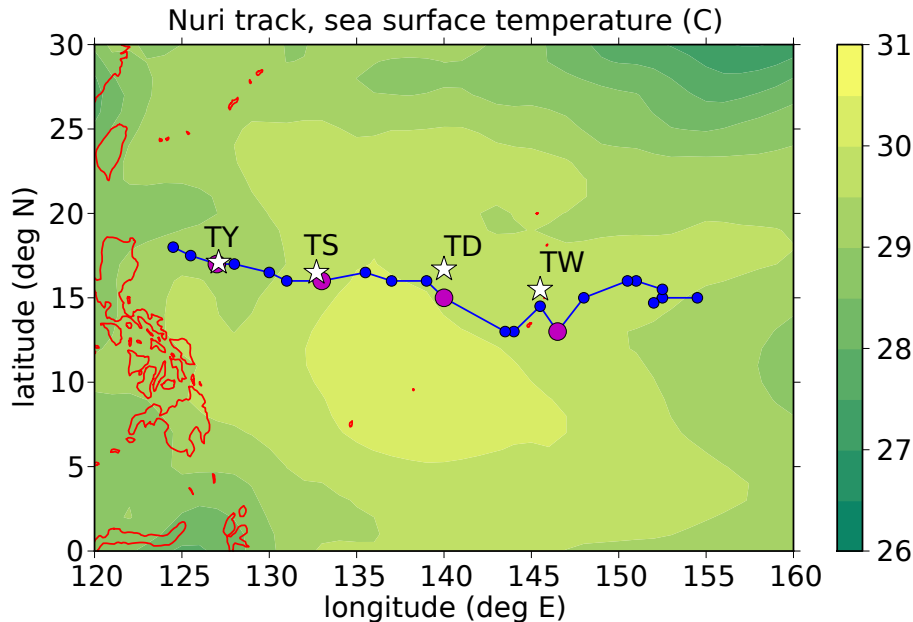


Fig. 1. Sea surface temperature and the observed low-level circulation centers of Nuri (white stars) during tropical wave (TW), tropical depression (TD), tropical storm (TS), and typhoon (TY) missions. The blue line indicates the track of the vorticity center in 850 hPa FNL data, with the blue dots spaced at 6 h intervals. The larger magenta dots indicate the 00:00 UTC FNL positions nearest to the reference times shown in Table 1 for the observational missions.

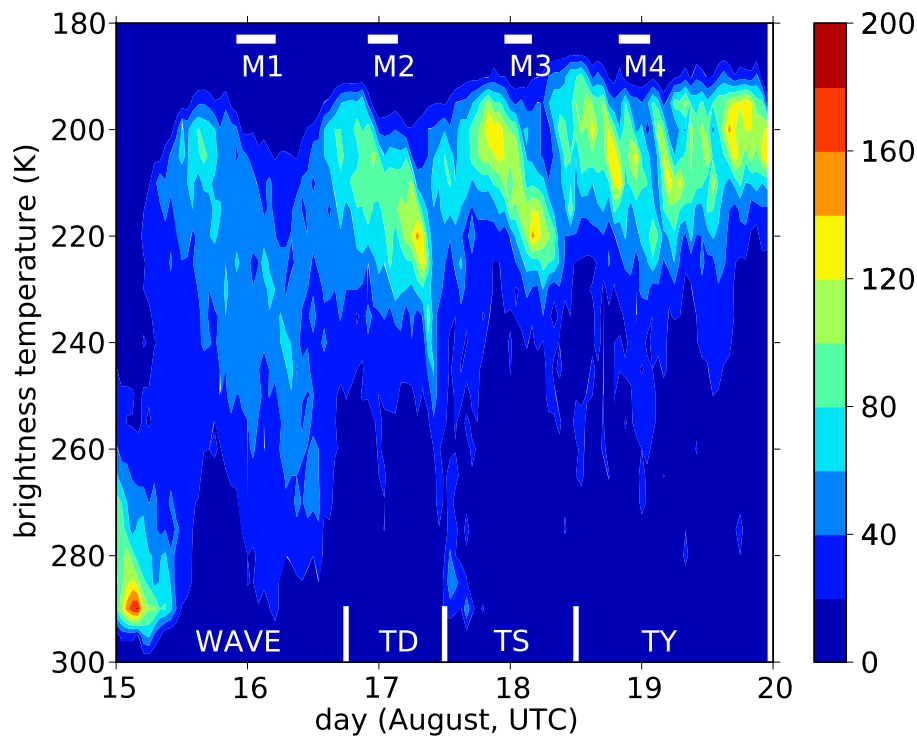


Fig. 2. Histogram of satellite infrared brightness temperatures of pixels in a $5^{\circ} \times 5^{\circ}$ square as a function of time, centered on tropical cyclone Nuri as it intensified. The stages of the storm (wave, tropical depression, tropical storm, typhoon) are shown, as well as the approximate times of the four aircraft missions, M1–M4 (see Table 1).

Vorticity budget in Typhoon Nuri

D. J. Raymond and
C. López Carrillo

Title Page

Abstract Introduction

Conclusions References

Tables Figures

◀ ▶

◀ ▶

Back Close

Full Screen / Esc

Printer-friendly Version

Interactive Discussion



Vorticity budget in Typhoon Nuri

D. J. Raymond and
C. López Carrillo

Title Page

Abstract

Introduction

Conclusions

References

Tables

Figures



Back

Close

Full Screen / Esc

Printer-friendly Version

Interactive Discussion

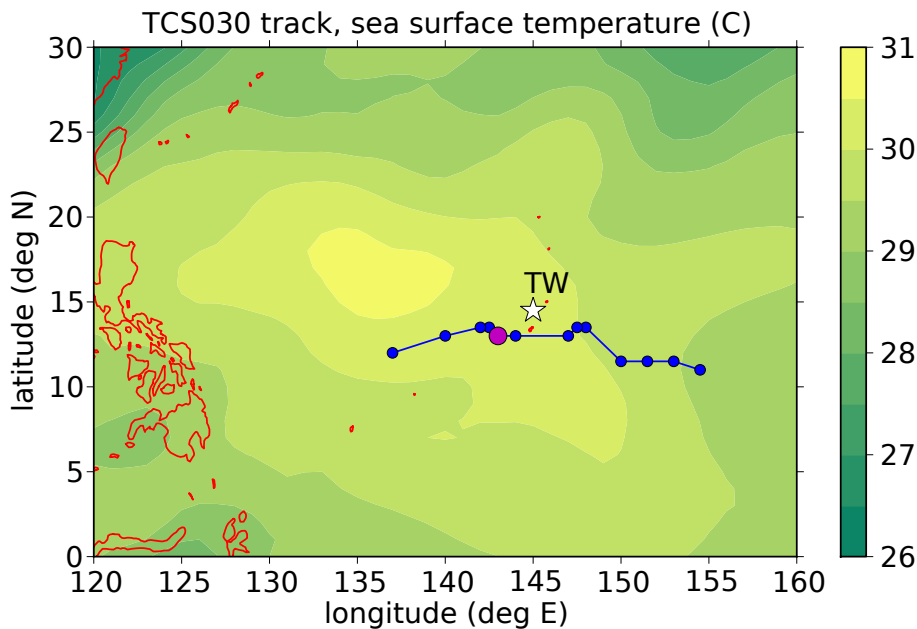


Fig. 3. As in Fig. 1 except for tropical wave TCS030.

Vorticity budget in Typhoon Nuri

D. J. Raymond and
C. López Carrillo

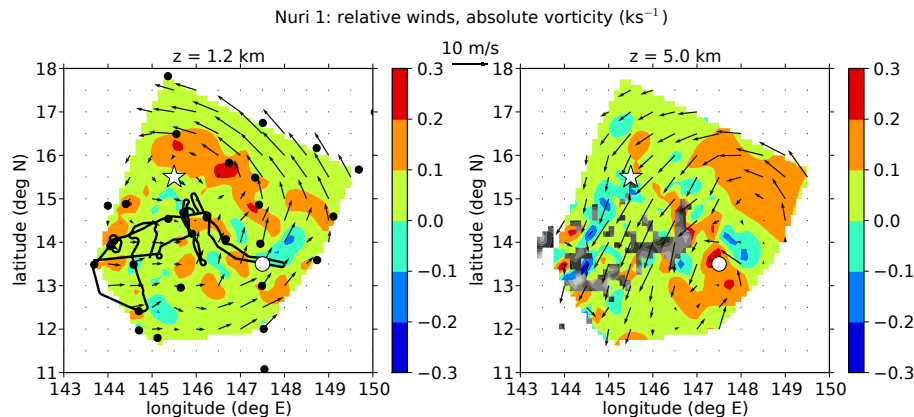


Fig. 4. Absolute vorticity (color levels) and storm-relative winds for Nuri mission 1 at 1.2 km (left panel) and 5 km (right panel). The black line and black dots in the left panel indicate the P-3 aircraft track and the locations of P-3 and WC-130J dropsondes. The gray scale insets in the right panel show regions of radar reflectivity exceeding 25 dBZ at 5 km. The white star and the white circle indicate the circulation centers in the PBL and at 5 km, respectively. The white areas reflect the geometry of the mask chosen for this mission.

[Title Page](#)
[Abstract](#)
[Introduction](#)
[Conclusions](#)
[References](#)
[Tables](#)
[Figures](#)
[◀](#)
[▶](#)
[◀](#)
[▶](#)
[Back](#)
[Close](#)
[Full Screen / Esc](#)
[Printer-friendly Version](#)
[Interactive Discussion](#)


Vorticity budget in Typhoon Nuri

D. J. Raymond and
C. López Carrillo

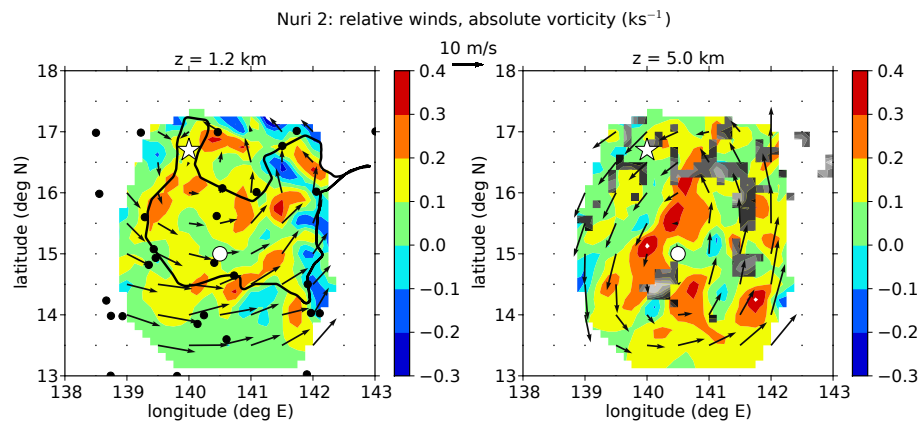


Fig. 5. As In Fig. 4 except second Nuri mission.

Title Page

Abstract

Introduction

Conclusions

References

Tables

Figures

◀

▶

◀

▶

Back

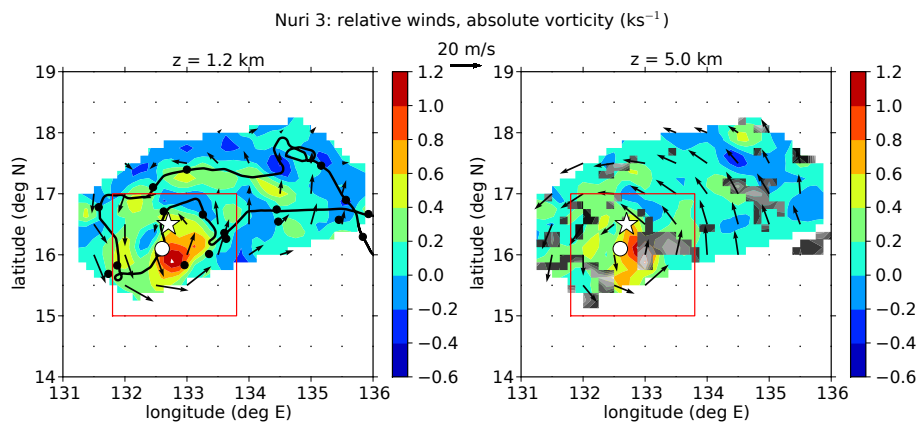
Close

Full Screen / Esc

Printer-friendly Version

Interactive Discussion



**Vorticity budget in
Typhoon Nuri**D. J. Raymond and
C. López Carrillo**Fig. 6.** As in Fig. 4 except third Nuri mission.

Title Page

Abstract

Introduction

Conclusions

References

Tables

Figures

◀

▶

◀

▶

Back

Close

Full Screen / Esc

Printer-friendly Version

Interactive Discussion



**Vorticity budget in
Typhoon Nuri**D. J. Raymond and
C. López Carrillo

Title Page

Abstract

Introduction

Conclusions

References

Tables

Figures

◀

▶

◀

▶

Back

Close

Full Screen / Esc

Printer-friendly Version

Interactive Discussion

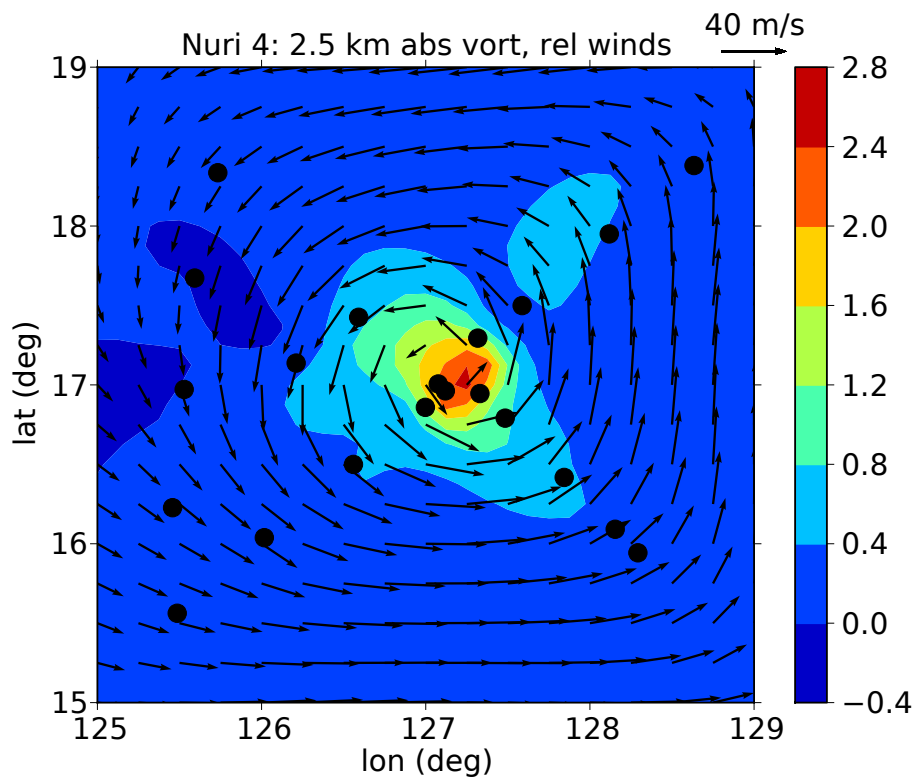


Fig. 7. Vorticity and storm relative winds at 2.5 km for the fourth Nuri mission (WC-130J dropsondes only). The black dots indicate dropsondes of sufficient quality to be used.

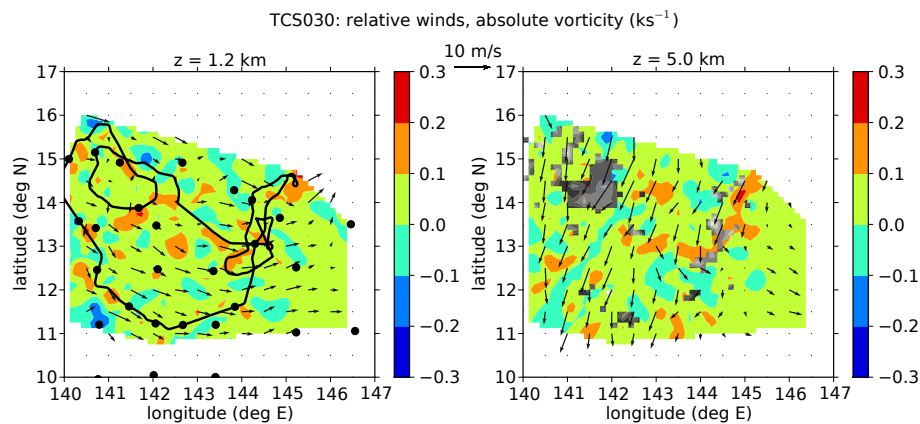
**Vorticity budget in
Typhoon Nuri**D. J. Raymond and
C. López Carrillo

Fig. 8. As in Fig. 4 except the TCS030 mission. No circulation centers are indicated.

Title Page

Abstract

Introduction

Conclusions

References

Tables

Figures

◀

▶

◀

▶

Back

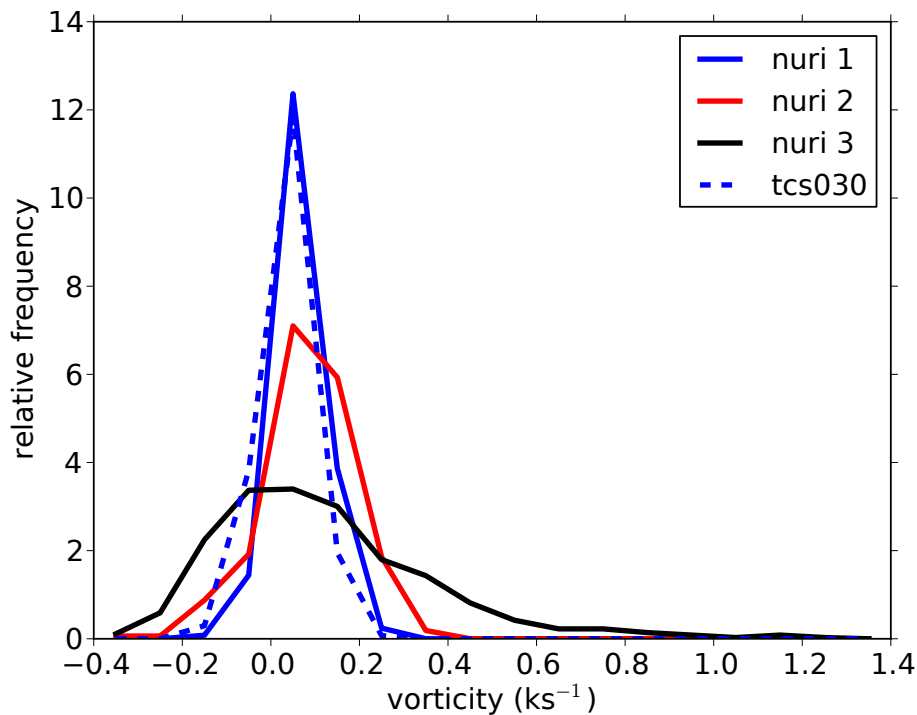
Close

Full Screen / Esc

Printer-friendly Version

Interactive Discussion



**Vorticity budget in
Typhoon Nuri**D. J. Raymond and
C. López Carrillo**Fig. 9.** Relative frequency of absolute vorticity values at 1.2 km in Figs. 4–6 and 8.[Title Page](#)[Abstract](#)[Introduction](#)[Conclusions](#)[References](#)[Tables](#)[Figures](#)[◀](#)[▶](#)[◀](#)[▶](#)[Back](#)[Close](#)[Full Screen / Esc](#)[Printer-friendly Version](#)[Interactive Discussion](#)

**Vorticity budget in
Typhoon Nuri**D. J. Raymond and
C. López Carrillo

Title Page

Abstract

Introduction

Conclusions

References

Tables

Figures

◀

▶

◀

▶

Back

Close

Full Screen / Esc

Printer-friendly Version

Interactive Discussion

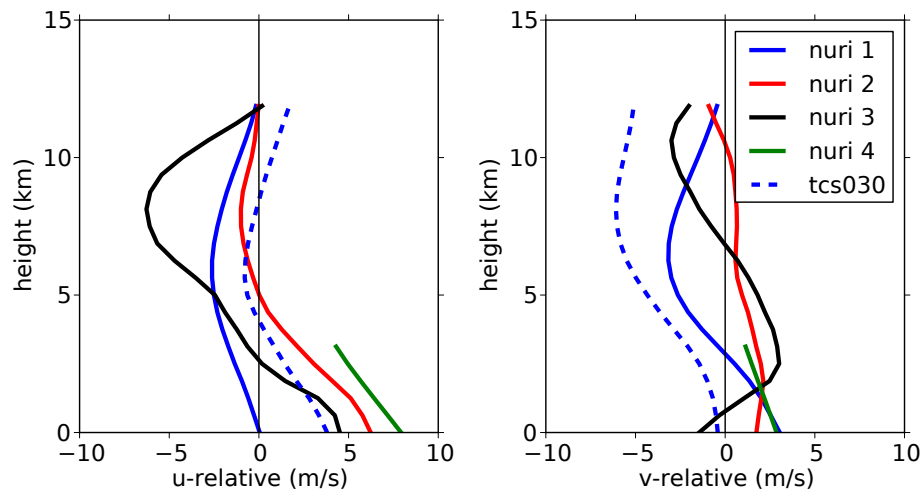


Fig. 10. Storm-relative westerly (left panel) and southerly (right panel) wind components for the four Nuri missions.

Vorticity budget in Typhoon Nuri

D. J. Raymond and
C. López Carrillo

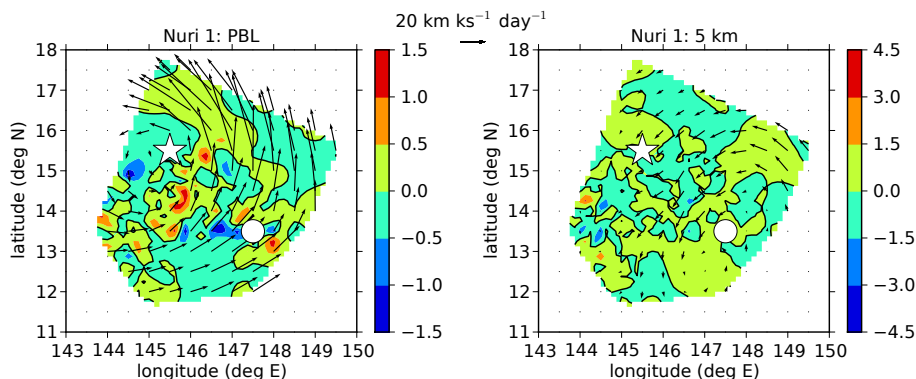


Fig. 11. Stretching tendency (filled contours) for vorticity and total vorticity flux (arrows) in the PBL ($0 < z < 1.2$ km; left panel) and at 5 km (right panel) as calculated from the analyzed wind fields for Nuri 1. The white stars (PBL) and circles (5 km) indicate the PBL storm-relative circulation center in and the black contours indicate zero stretching tendency. The vorticity flux has been low-pass filtered with a filter length of 0.5° for clarity of the overall pattern, but the stretching tendency has not. Note the different scales between the plots.

Title Page

Abstract

Introduction

Conclusions

References

Tables

Figures

◀

▶

◀

▶

Back

Close

Full Screen / Esc

Printer-friendly Version

Interactive Discussion



Vorticity budget in Typhoon Nuri

D. J. Raymond and
C. López Carrillo

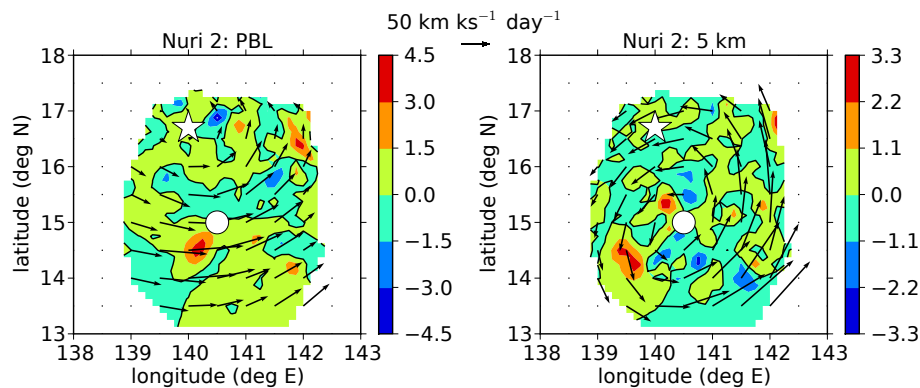


Fig. 12. As in Fig. 11 except for Nuri 2.

Title Page

Abstract Introduction

Conclusions References

Tables Figures

◀ ▶

◀ ▶

Back Close

Full Screen / Esc

Printer-friendly Version

Interactive Discussion



Vorticity budget in Typhoon Nuri

D. J. Raymond and
C. López Carrillo

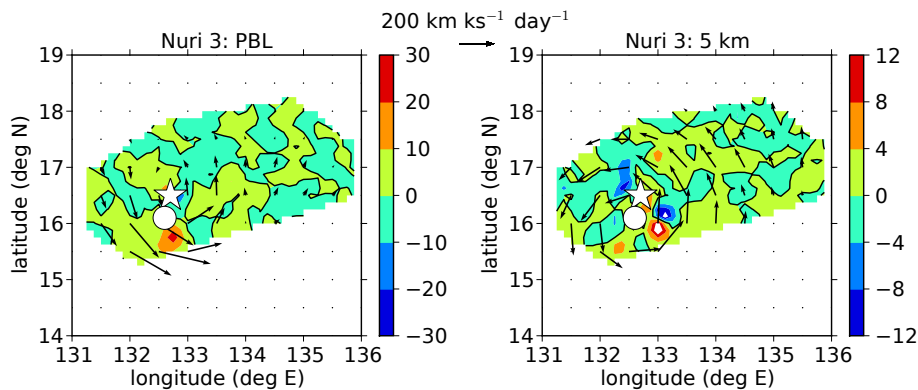


Fig. 13. As in Fig. 11 except for Nuri 3.

Title Page

Abstract

Introduction

Conclusions

References

Tables

Figures

◀

▶

◀

▶

Back

Close

Full Screen / Esc

Printer-friendly Version

Interactive Discussion



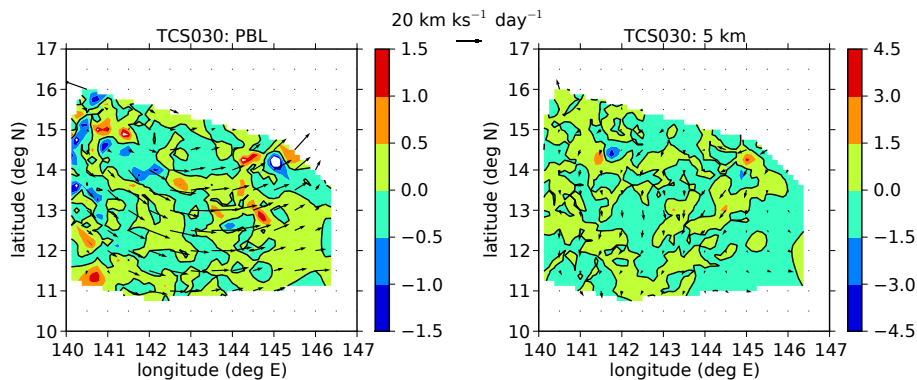
**Vorticity budget in
Typhoon Nuri**D. J. Raymond and
C. López Carrillo

Fig. 14. As in Fig. 11 except for TCS030. No circulation centers are shown in this case.

Title Page

Abstract

Introduction

Conclusions

References

Tables

Figures

◀

▶

◀

▶

Back

Close

Full Screen / Esc

Printer-friendly Version

Interactive Discussion



Vorticity budget in Typhoon Nuri

D. J. Raymond and
C. López Carrillo

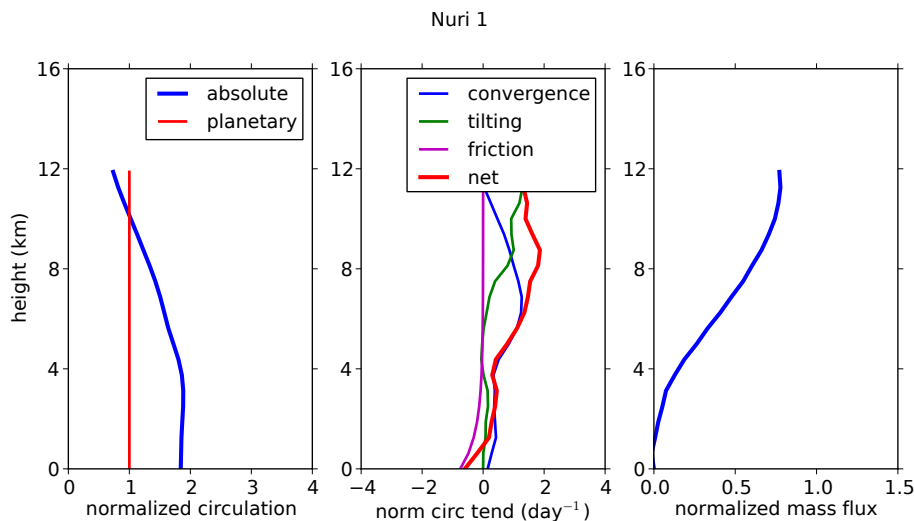
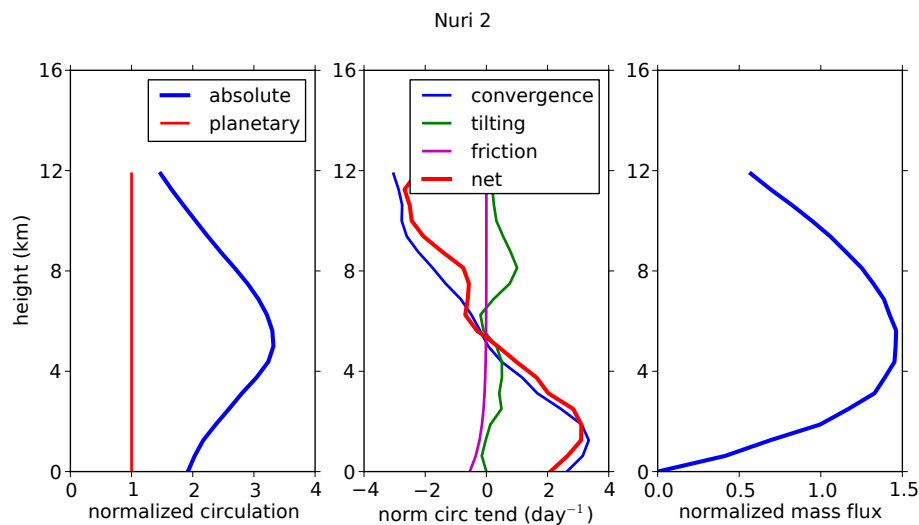


Fig. 15. Nuri 1 vertical profiles integrated over the analyzed region shown in Fig. 4. Left panel: Planetary (red) and absolute (blue) circulations. Middle panel: Contributions to the total circulation tendency (red) due to vorticity convergence (blue), vortex tilting (green), and surface friction (magenta). Right panel: Vertical mass flux profile. All curves are divided by the planetary circulation for normalization purposes.

[Title Page](#)
[Abstract](#)
[Introduction](#)
[Conclusions](#)
[References](#)
[Tables](#)
[Figures](#)
[⏪](#)
[⏩](#)
[◀](#)
[▶](#)
[Back](#)
[Close](#)
[Full Screen / Esc](#)
[Printer-friendly Version](#)
[Interactive Discussion](#)


**Vorticity budget in
Typhoon Nuri**D. J. Raymond and
C. López Carrillo**Fig. 16.** As in Fig. 15 except Nuri 2 (Fig. 5).

Title Page

Abstract

Introduction

Conclusions

References

Tables

Figures

◀

▶

◀

▶

Back

Close

Full Screen / Esc

Printer-friendly Version

Interactive Discussion



Vorticity budget in Typhoon Nuri

D. J. Raymond and
C. López Carrillo

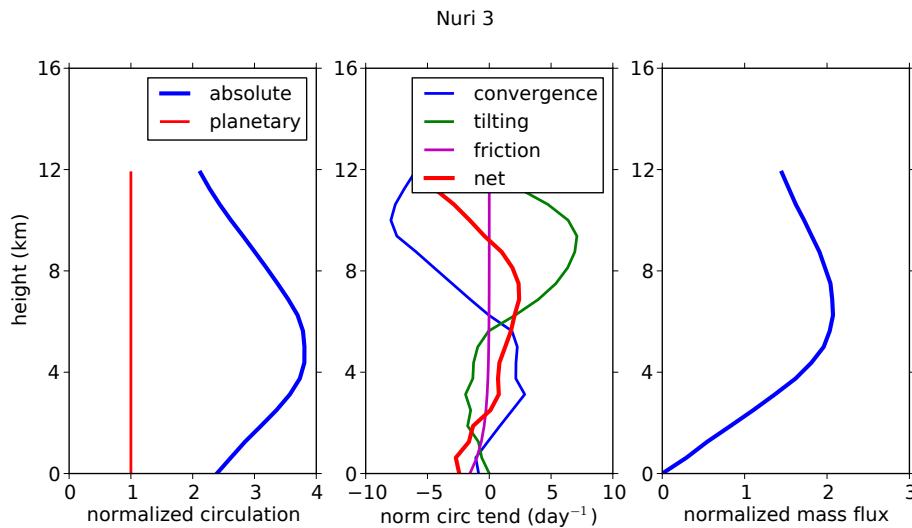


Fig. 17. As in Fig. 15 except Nuri 3 (Fig. 6).

Title Page

Abstract Introduction

Conclusions References

Tables Figures

◀ ▶

◀ ▶

Back Close

Full Screen / Esc

Printer-friendly Version

Interactive Discussion



Vorticity budget in Typhoon Nuri

D. J. Raymond and
C. López Carrillo

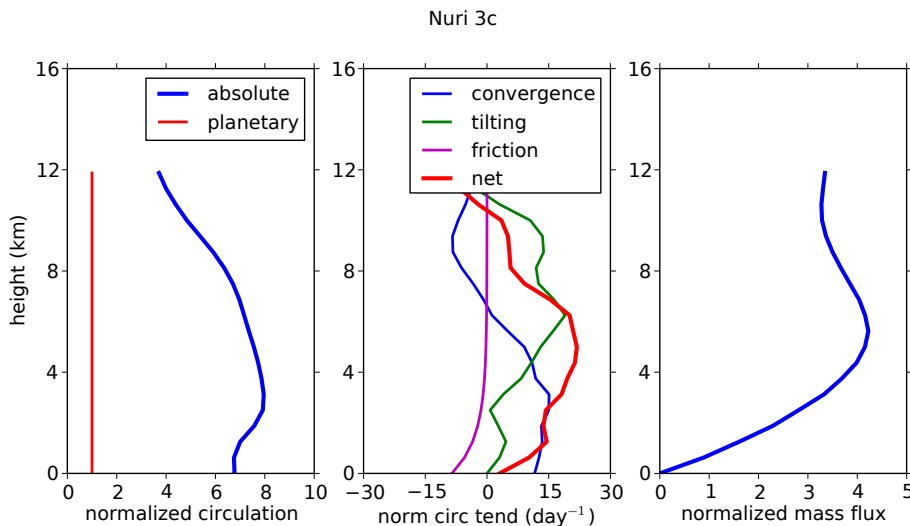


Fig. 18. As in Fig. 17 except for integration over a 2°-square box centered on the core of Nuri 3.

Title Page

Abstract Introduction

Conclusions References

Tables Figures

◀ ▶

◀ ▶

Back Close

Full Screen / Esc

Printer-friendly Version

Interactive Discussion



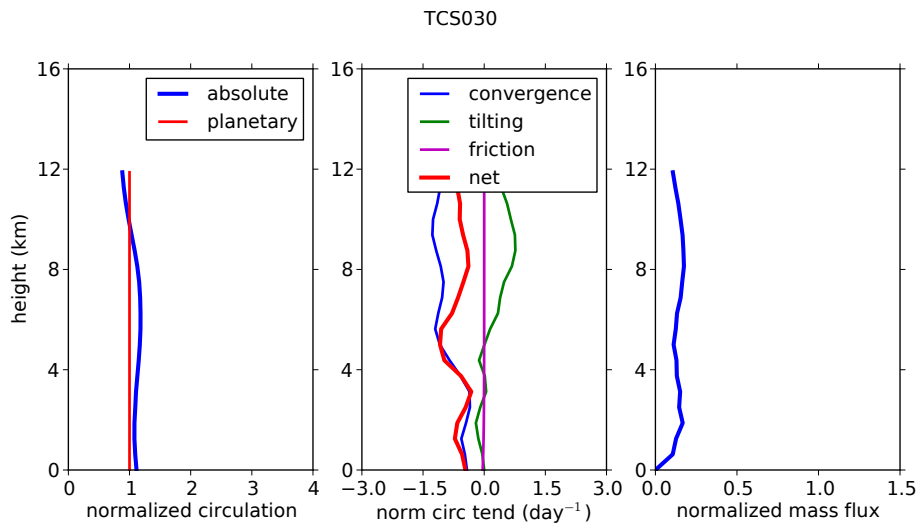
**Vorticity budget in
Typhoon Nuri**D. J. Raymond and
C. López Carrillo

Fig. 19. As in Fig. 15 except TCS030 (Fig. 8).

[Title Page](#)[Abstract](#)[Introduction](#)[Conclusions](#)[References](#)[Tables](#)[Figures](#)[◀](#)[▶](#)[◀](#)[▶](#)[Back](#)[Close](#)[Full Screen / Esc](#)[Printer-friendly Version](#)[Interactive Discussion](#)

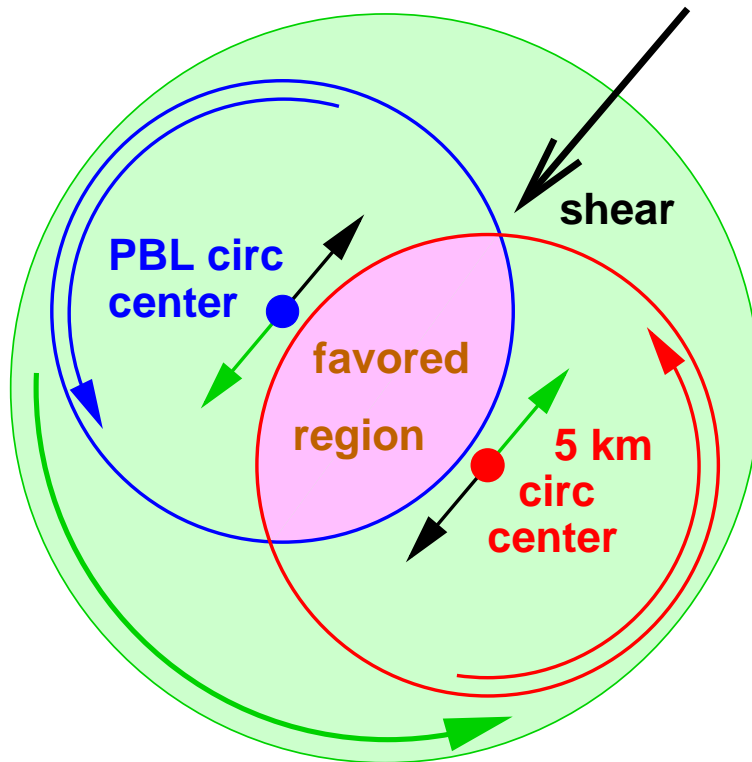


Fig. 20. Interaction of shear (thick black vector) with a broad region of positive relative vorticity (large green circle). The circulation centers in the PBL and at 5 km are located where the system-relative ambient winds at the respective levels (black arrows) just balance the induced circulation from the vorticity pattern (green arrows). The blue and red circles represent the limits of closed circulation streamlines in the PBL and at 5 km. The magenta-colored region of overlap between these circles represents the region where the entire column between the PBL and 5 km is protected from incursions of environmental air.

Vorticity budget in Typhoon Nuri

D. J. Raymond and
C. López Carrillo

Title Page

Abstract

Introduction

Conclusions

References

Tables

Figures

◀

▶

◀

▶

Back

Close

Full Screen / Esc

Printer-friendly Version

Interactive Discussion

